metals

MDPI

Article

Hydrogen Embrittlement Susceptibility of R4 and R5 High-Strength Mooring Steels in Cold and Warm Seawater

Garikoitz Artola [1,2,*], Alberto Arredondo [3], Ana Isabel Fernández-Calvo [2] and Javier Aldazabal [1]

[1] Tecnun, University of Navarra, Manuel de Lardizábal 15, 20018 San Sebastián, Spain; jaldazabal@tecnun.es
[2] IK4-AZTERLAN, Research and Development of Metallurgical Processes, Aliendalde Auzunea 6, 48200 Durango, Spain; afernandez@azterlan.es
[3] Vicinay Marine Innovación, Ibaiondo 1, 48940 Leioa, Bizkaia, Spain; aarredondo@vicinayinnovacion.com
* Correspondence: gartola@azterlan.es; Tel.: +34-94-621-54-70

Received: 7 August 2018; Accepted: 4 September 2018; Published: 6 September 2018

Abstract: Hydrogen embrittlement susceptibility ratios calculated from slow strain rate tensile tests have been employed to study the response of three high-strength mooring steels in cold and warm synthetic seawater. The selected nominal testing temperatures have been 3 °C and 23 °C in order to resemble sea sites of offshore platform installation interest, such as the North Sea and the Gulf of Mexico, respectively. Three scenarios have been studied for each temperature: free corrosion, cathodic protection and overprotection. An improvement on the hydrogen embrittlement tendency of the steels has been observed when working in cold conditions. This provides a new insight on the relevance of the seawater temperature as a characteristic to be taken into account for mooring line design in terms of hydrogen embrittlement assessment.

Keywords: SSRT; hydrogen embrittlement; high-strength steel; cathodic protection; mooring; sea temperature effect

1. Introduction

The increase in the use of high-strength steels in key structural elements is a matter of interest for offshore and subsea applications since many years [1]. Taking advantage of their increased specific strength allows for downsizing structures, saving weight, costs and reducing the number of elements required for a given structural function [2]. As a drawback, high-strength steels must be handled with care in marine service as they are susceptible to environmental embrittlement. In this context, cathodic protection, which is a widespread countermeasure against the corrosive action of seawater, is a major factor to be taken into account since it enhances Hydrogen Embrittlement (HE) phenomena in these steels.

Hydrogen can lead to several hydrogen-induced damage types in metallic alloys, namely: HE, hydrogen-induced blistering, cracking from precipitation of internal hydrogen, hydrogen attack and cracking from hydride formation [3]. The degradation mechanism of interest in this work, HE, is related to the interference of diffusible hydrogen with dislocation behaviour. This interference determines both the local hydrogen concentration and stress field, making high-strength steels more prone to undergo brittle fracture instead of following a ductile response [4].

HE failures are characterized by a sudden brittle fracture [5] and, in consequence, the combination of high-strength steels and cathodic protection must be assessed to avoid structural safety incidents in offshore structures that may lead to significant economic and ecologic loses.

The risk of unexpected failure can be reduced by periodically monitoring the health of the high-strength steel components. The assessment of the loss of resistant section caused by corrosion and the presence of HE cracking can be used to decide on component replacement or repair. Dry dock inspection is not feasible though in all cases. Elements such as the legs of production jack-ups and the mooring chains fall in this type of components [6,7], where dry docking is not feasible and in-site inspection is difficult.

To account for this problem, regulatory actions have been taken that reduce the risk of HE failure. In the case of mooring lines, standards that regulate design and qualification include HE related controls. More specifically, approval programmes for high-strength mooring chains require Slow Strain Rate Tensile (SSRT) testing to assess HE susceptibility [8]. These steels are classified into six grades according to their minimum specified ultimate tensile strength: R3, R3S, R4, R4S, R5 and R6 (Table 1). The choice of SSRT testing is due to its ability to provide quick and cost-effective screening and comparison to study the resistance of materials against HE in different environmental conditions. SSRT testing allows calculating several embrittlement indexes, which are the ratio between the values of strength or ductility in the conditions of interest and a control condition [9]. For example, finished chain components, R4S, R5 and R6, require dry air as control condition.

The conditions of interest vary among the grades: free corrosion in synthetic seawater according to ASTM D1141 is used for R4S and R5 grades while for R6, not only free corrosion testing is required, but also employing cathodic protection of −850 mV and overprotection of −1200 mV. It is well known that the different offshore locations in the world lead to different seawater conditions, among which the water temperature can be considered to vary between 3 °C and 23 °C [10]. However, SSRT testing for qualification of mooring chains in both situations is performed at room temperature. The seawater temperature influences factors such as the hydrogen transport in the electrolyte, presence of dissolved oxygen or hydrogen absorption rate that drive the hydrogenation rate of the steel and influence the result of the SSRT testing. Being the temperature a key factor in electrolytic reactions, the question that arises is whether HE susceptibility of the mooring steels changes from cold to warm seas or not.

Table 1. Minimum required mechanical properties of steel grades for mooring chains and accessories [11].

Grade	Yield Strength Rp0.2 (MPa)	Ultimate Tensile Strength Rm (MPa)	Elongation E (%)	Reduction in Area RA (%)
R3	>410	>690	>17	>50
R3S	>490	>770	>15	>50
R4	>580	>860	>12	>50
R4S	>700	>960	>12	>50
R5	>760	>1000	>12	>50
R6	>900	>1100	>12	>50

Despite HE is a relevant design factor for high-strength steels and there is plenty of SSRT testing based works in the literature [12–17], steel grades and testing conditions show a wide variety (some authors employ straight specimens, others use notched specimens; some works employ hydrogen pre-charging, others study in service re-embrittlement) and none answers the question above concerning the effect of seawater temperature. The work which is presented here is aimed to answer it for high yield strength mooring chain link R4 and R5 steels and R4 mooring accessory steel, under different applied potentials (free corrosion, −850 and −1200 mV), in submerged service in cold (3 °C) and warm (23 °C) seawater.

2. Materials and Methods

The materials employed for the study were ready-to-use mooring chain links and accessories according to Figure 1 and Table 2. The two R4 samples (A and B) distinguish from each other due to the typology of product. Sample A was a chain link, while sample B was a chain accessory. The R5

grade corresponded to a chain link sample. All the three steels were vacuum degassed during their production process. The dimensions of the samples ranged from Ø160 to Ø200 mm.

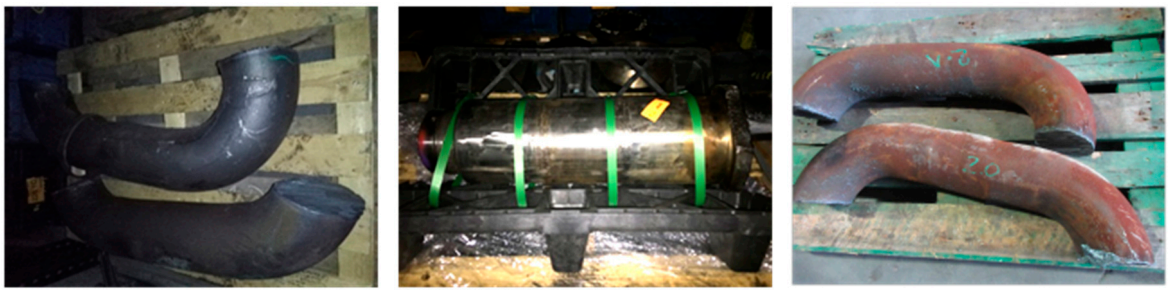

Figure 1. Left to right, samples A, B and C. **Sample A**: Two R4 chain link halves; **Sample B**: R4 Chain accessory; **Sample C**: Two R5 chain link halves.

Table 2. Identification of the three high-strength materials tested in the study.

Identification	Grade	Component	Section (mm)
A	R4	Chain link	Ø160
B	R4	Accessory	Ø200
C	R5	Chain link	Ø160

A set of 22 tensile specimens machined according to UNE EN-ISO 6892-1 (Figure 2) was employed for the HE survey of each sample. All the specimens were obtained from regions as close as possible to the surface of each sample. In all cases the distance between the specimen and the skin of the link or the accessory was less than 30 mm.

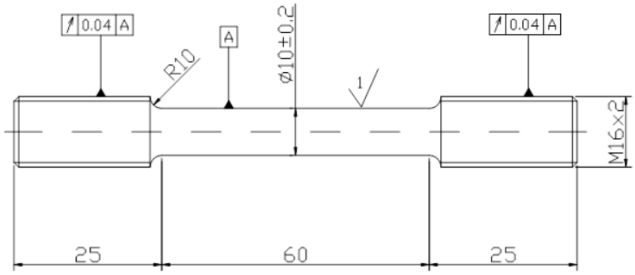

Figure 2. Tensile specimen geometry employed for the testing (dimensions in mm).

A 100 kN tensile testing machine (Mod. 1475, Zwick Roell AG, Ulm, Germany) was used for the experimental work. One conventional tensile test according UNE EN ISO 6892-1 was performed (see Table 3) per each material to ensure that the resistance grades were correct according to Table 1. As shown in the Table 3, in practice, both R4 and R5 grades widely surpass the minimum yield strength requirement of 580 MPa specified in the standards. The rest of the specimens were employed for carrying out 3 SSRT tests per material (A, B, C) in each of the 7 different conditions listed in Table 4. It is remarkable that the yield strengths were in all cases well above the minimum required values for each grade. The testing speed was kept constant for all SSRT tests and equal to 0.03 mm/min (straining speed of 10^{-5} s^{-1} as stated in [11]).

The chosen electrolyte for submerged tests was a substitute for seawater prepared according to ASTM D1141-98(2013), in the version that includes heavy metals. A volume of 600 mL of the preparation was used in each submerged test. In these tests, the specimen's calibrated zone was completely covered with water. The temperature control of the tests was attained by placing the seawater container in a water bath (Figure 3) that was equipped with an immersion chiller

(Frigedor-reg, JP Selecta S.A., Abrera, Spain). The achieved temperature control, measured with a type K thermocouple on the surface of the tensile specimen, was ±2 °C the target temperature set point.

Table 3. Verification of the strength grade of the three materials, including the extended uncertainty for each measurement (K = 2).

Identification	Rp0.2 (MPa)	Rm (MPa)	E (%)	RA (%)
A	810 ± 9	890 ± 9	18.0 ± 1.5	71 ± 1
B	810 ± 9	905 ± 9	19.0 ± 1.5	67 ± 1
C	980 ± 10	1035 ± 10	15.0 ± 1.5	59 ± 1

Table 4. Testing conditions.

Condition	Description	Environment	Temperature (°C)	Cathodic Protection (mV)
AI	Air	Air	23	–
FC-C	Free Corrosion	Seawater substitute	3	–
FC-W	Free Corrosion	Seawater substitute	23	–
CP-C	Cathodic Protection	Seawater substitute	3	−850
CP-W	Cathodic Protection	Seawater substitute	23	−850
OP-C	Overprotection	Seawater substitute	3	−1200
OP-W	Overprotection	Seawater substitute	23	−1200

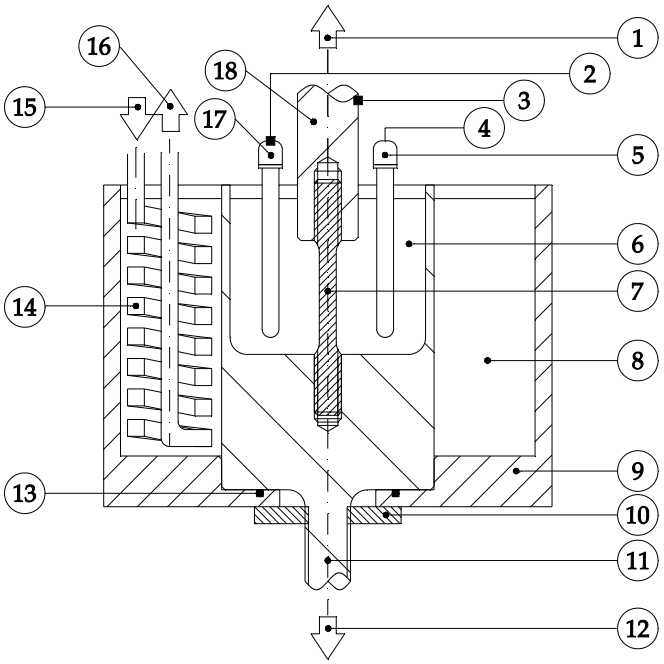

Figure 3. Testing scheme for Slow Strain Rate Tensile (SSRT) tests carried out in seawater substitute at IK4-AZTERLAN facilities. (1. Connection to the testing machine. 2. Connection to the multi-meter. 3. Connection to the voltage source and the multi-meter. 4. Connection to the voltage source. 5. Graphite electrode. 6. Seawater substitute. 7. SSRT test specimen. 8. Water bath. 9. Water bath container. 10. Fixing nut for the water bath. 11. Lower fixture and seawater container. 12. Connection to the testing machine. 13. O-ring. 14. Water bath chilling coil. 15. Refrigerating fluid entrance to the coil. 16. Refrigerating fluid exit from the coil. 17. Ag/AgCl reference electrode. 18. Upper fixture.).

For the testing under cathodic protection, a graphite electrode was connected to a conventional DC power source (Agilent Technologies, Santa Clara, CA, USA). The applied potential was controlled

with an Ag/AgCl electrode and kept within ±25 mV from the set-points during the tests under cathodic protection and overprotection.

A macroscopic assessment of the hydrogen induced cracking phenomena was performed on the fractured SSRT specimens by visual inspection of the necking area.

3. Results and Discussion

The average values for strength and ductility related properties obtained from the SSRT testing are gathered in Table 5. The experimental deviations on the averages are calculated for a confidence interval of 95% following the equation:

$$IC95 = \pm\sqrt{(U(K=2))^2 + \left(\frac{t_{\alpha=0.05,2}S_v}{\sqrt{3}}\right)^2} \quad (1)$$

where U (K = 2) is the measurement uncertainty of the individual tests employed to calculate the average, $t_{\alpha\,=\,0.05,2}$ is Student's t for a level of significance of 0.05 and 2 degrees of freedom and S_v is the experimental standard deviation of the data.

Table 5. Average of the mechanical properties measured by SSRT on the three materials.

Sample	Condition	Rp 0.2 (MPa)	Rm (MPa)	E (%)	RA (%)
A	AI	800 ± 13	878 ± 12	18.3 ± 1.7	71.3 ± 1.6
A	FC-C	815 ± 32	887 ± 17	18.2 ± 3.0	72.0 ± 1.0
A	FC-W	803 ± 16	884 ± 27	17.7 ± 2.2	69.7 ± 3.9
A	CP-C	793 ± 60	883 ± 13	17.4 ± 2.1	53.0 ± 10.9
A	CP-W	809 ± 16	878 ± 10	14.8 ± 3.2	45.3 ± 3.9
A	OP-C	812 ± 33	892 ± 13	14.4 ± 5.0	43.3 ± 15.2
A	OP-W	800 ± 10	883 ± 10	11.5 ± 1.5	32.0 ± 10.1
B	AI	804 ± 77	903 ± 68	19.1 ± 2.2	68.0 ± 4.4
B	FC-C	798 ± 85	897 ± 45	18.2 ± 2.0	67.3 ± 3.9
B	FC-W	816 ± 52	914 ± 47	18.7 ± 2.3	65.0 ± 1.7
B	CP-C	784 ± 35	884 ± 17	16.3 ± 5.4	54.0 ± 13.9
B	CP-W	809 ± 37	903 ± 13	17.0 ± 4.1	54.0 ± 17.4
B	OP-C	809 ± 93	911 ± 74	15.6 ± 1.7	41.0 ± 6.6
B	OP-W	797 ± 65	894 ± 36	15.2 ± 4.5	42.3 ± 18.7
C	AI	971 ± 61	1026 ± 14	16.0 ± 4.4	59.7 ± 1.7
C	FC-C	985 ± 109	1035 ± 25	15.3 ± 2.9	59.7 ± 7.2
C	FC-W	963 ± 80	1025 ± 20	14.6 ± 3.6	59.0 ± 2.7
C	CP-C	1020 ± 23	1044 ± 10	14.1 ± 1.5	48.0 ± 7.5
C	CP-W	968 ± 43	1022 ± 14	13.5 ± 2.5	40.0 ± 19.4
C	OP-C	1017 ± 17	1044 ± 10	9.7 ± 3.6	29.3 ± 14.4
C	OP-W	993 ± 20	1027 ± 16	7.3 ± 3.5	24.0 ± 12.5

The table allows performing two observations without requiring more elaboration. On one hand, the SSRT tests performed in air (AI) and under free corrosion, both in cold and warm water (FC-C and FC-W), resemble the results that were obtained in conventional tensile tests, no matter of the steel grade. This means that none of the steels shows a significant HE susceptibility for the sole reason of being immersed in seawater. Thus, the discussion in the following is focused in the cathodically protected testing conditions.

On the other hand, yield strength and ultimate tensile strength show small variations for each steel grade. This discards strength related data, which is used for SSRT assessment when notched specimens are employed [14,15], for the further study of the results.

3.1. Influence of the Applied Cathodic Potential and the Temperature in the Embrittlement

The evaluation of the HE produced in the cathodically protected specimens has been based on Plastic Elongation Ratio ($RE_{COND/CONT}$) and the Reduction in Area Ratio ($RRA_{COND/CONT}$), which are calculated as (2) and (3) [9]:

$$RE_{COND/CONT} = E_{COND}/E_{CONT} \quad (2)$$

$$RRA_{COND/CONT} = RA_{COND}/RA_{CONT} \quad (3)$$

where E_{COND} and RA_{COND} are the average elongation and reduction in area of the SSRT tests in each condition of interest; and E_{CONT} and RA_{CONT} stand for the average of the SSRT test results in the control condition. This gives a measure of the ductility drop in E and RA which is relative to the control condition.

Table 6 and Figure 4 show the HE ratios of the tests under cathodic protection for a control condition of the SSRT tests in air (AI). Figure 4 HE stays in close proximity or degrades when SSRT is carried out in warm seawater, in comparison to cold water. For samples A and C, the embrittlement ratios actually degrade for the warm testing, while they remain nearly constant for sample B. This observation confirms that the temperature of the seawater affected to HE susceptibility measurements for the offshore grade high-strength steel samples that were tested. The improvement at low temperatures can't be explained in terms of the physical properties of the steel, as only minor changes were observed under free corrosion both with cold and warm water. Hydrogen solubility and diffusivity in the studied steels shouldn't change drastically [18] between 3 °C and 23 °C. Thus, the drop in RE and RRA ratios for samples A and C is likely to be related to changes in the physical properties of the seawater from cold to warm condition [19]. Temperature changes affect electrolytic behavior due to their influence on oxygen concentration [10,20], pH [21] and electrolyte activity [22].

Table 6. Hydrogen Embrittlement (HE) assessment ratios for the underwater cathodically protected testing.

Sample	Condition	$RE_{COND/AI}$	$RRA_{COND/AI}$
A	CP-C	95%	74%
A	CP-W	81%	64%
A	OP-C	79%	61%
A	OP-W	63%	45%
B	CP-C	83%	76%
B	CP-W	89%	79%
B	OP-C	80%	60%
B	OP-W	83%	62%
C	CP-C	88%	80%
C	CP-W	84%	67%
C	OP-C	61%	49%
C	OP-W	45%	40%

When comparing the ratios for A-CP-W and A-OP-C, it is noticeable that the increase in testing temperature had nearly the same effect in RRA and RE as keeping the temperature low and increasing the applied potential. This result points out that the detrimental effect of increasing the temperature can be as strong as the effect of increasing the potential for SSRT testing in cold water. This observation is not extensible to materials B and C.

The expected trend on HE susceptibility (a decrease in ductility as the applied voltage is increased) was found in all cases except for elongation ratios for sample B. For this sample, the accessory R4 grade, the increase from −850 mV to −1200 mV only led to a small drop in elongation. This implies that R4 grade can show resistance to HE even for high yield strength samples and aggressive cathodic protection. Figure 4 also shows that, considering overall behaviour, sample B showed the lowest HE susceptibility among the three materials.

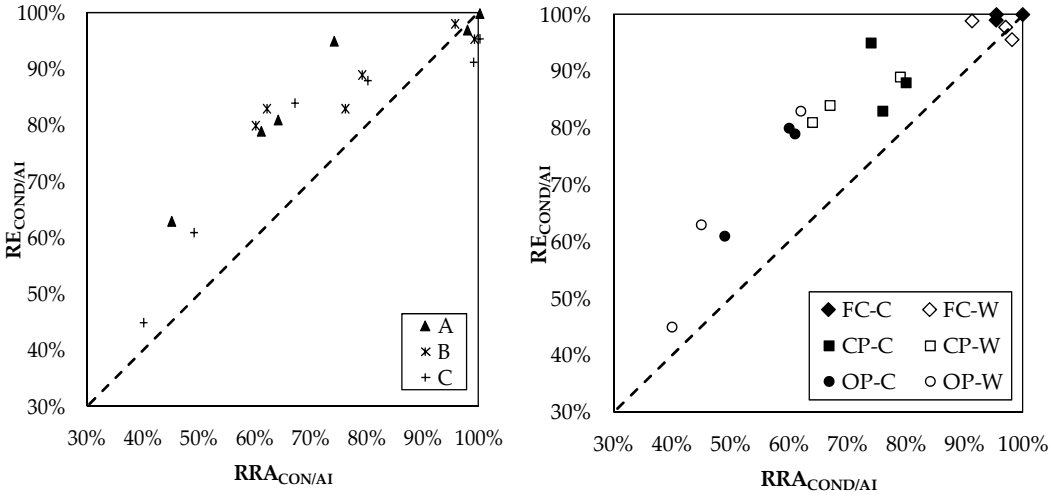

Figure 4. HE ratios for all the underwater testing conditions, with AI as control condition. Left to right: Points labelled by different material and by different SSRT conditions.

3.2. Comparison between Steel Grades

Taking the E and RA results from sample B as the control value to re-calculate the HE ratios, allows employing results from identical testing conditions to compare the three materials (Figure 5). The comparison between samples requires a modification in the calculation criteria, since otherwise the initial E and RA differences between grades would introduce a fake embrittlement effect even in AI condition. Thus, the values for the ratios of samples A and C in Figure 5 have been normalized by the initial E and RA ratios relative to B in air as detailed in (4) and (5):

$$RE_{C\text{-}COND/B\text{-}COND} = (E_{C\text{-}COND}/E_{B\text{-}COND})/(E_{C\text{-}AI}/E_{B\text{-}AI}) \quad (4)$$

$$RRA_{C\text{-}COND/B\text{-}COND} = (RA_{C\text{-}COND}/RA_{B\text{-}COND})/(RA_{C\text{-}AI}/RA_{B\text{-}AI}) \quad (5)$$

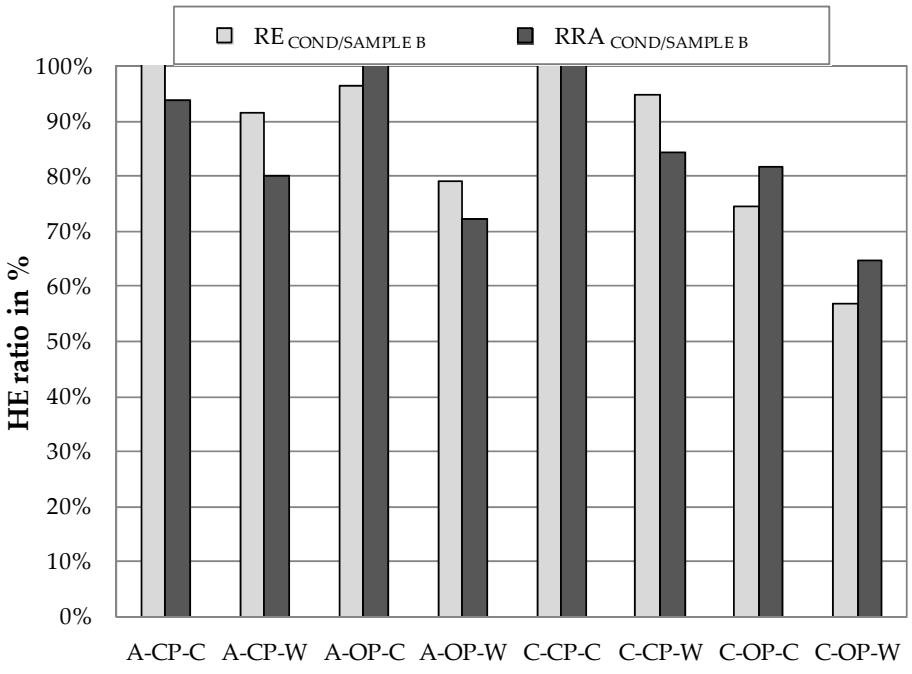

Figure 5. HE ratios with the average value obtained in each condition for material B as control reference.

It can be observed again that the tests in cold water lead to better HE response, despite the control condition has changed from the one employed for Figure 4. This similitude between both figures is explained by the low sensitivity of the reference material (sample B) to the testing temperature changes.

Regarding the back-to-back comparisons between the samples, the HE ratios of sample A to sample B give similar results in cold seawater, both for −850 mV and −1200 mV cathodic protection potentials. For the results in warm water though, the R4 chain link steel showed lower SSRT ratios than the R4 accessory steel. This difference in the behaviour for two steels belonging to the same R4 grade is explained by the fact that mooring chain steel grades are not related to a narrow specification of chemical composition, production process or heat treatment, but to a set of minimum mechanical properties [11]: two R4 grade components are not necessarily made of equivalent steels.

Shifting to the comparison between C and B, it should be expected to find lower HE ratios than in the comparison between A and B, since in general, higher strength steels are considered more susceptible to HE. It is thus noticeable that, when the ratios are normalized to the initial E and RA ratios relative to B in air, there is not a clear advantage between samples A and C. Depending on the condition which is analyzed, sample C can show less relative HE susceptibility than sample A. This is true for the CP condition, while for OP the results point the other way round. According to these results, a R5 grade steel can stand HE as well as a R4 grade steel under cathodic protection of −850 mV, what is generally accepted as the design protective potential for low alloy steels [23]. This enhances the interest of employing higher strength grades in mooring lines.

3.3. Macroscopic Assessment of the Hydrogen Induced Cracking

The visual inspection of the necking area of the SSRT specimens showed two clear patterns depending on the steel grade (Figure 6), which were most clearly distinguished in OP condition:

- Sample A developed a pattern of multiple short cracks all around the necking area. The metallographic cross section A-A across the longitudinal axis of the specimen, indicated in Figure 6 Material A, confirms the accumulation of several short cracks, very close to each other, in the neighbourhood of the necking (Figure 6, bottom-left). This behaviour can be interpreted as hydrogenation all around the necking area, prior to the concentration of the damage in the cracks that grew faster and led to the specimen failure.
- Samples B and C on the other hand showed very few cracks. The metallographic cross section B-B, performed as section A-A, confirms the lower density of cracks that are, in turn, longer (Figure 6, bottom right). In terms of hydrogenation this is related to a quicker hydrogen intake and diffusion in the tip of the first few cracks that nucleated in the specimen. In this sense, sample B and C behaved in a similar manner.

These observations are relevant if NDT techniques are intended to be applied for assessing the health of mooring lines. Both the most commonly employed underwater techniques (visual and magnetic particle inspection) [24] and the less extended (e.g., ultrasound and acoustic emission based) [7,25] are more efficient if the expected morphology of the defect is known. This holds true even if the use of algorithms combining data from different NDT methods is considered [26]. An earlier detection of HE cracking should be expected in Materials B and C, since the few cracks growing would reach the resolution threshold of the NDT techniques earlier than the distributed damage of Material A. The change in the cracking pattern between the two R4 grades is attributed to the differences in the product types that were chosen for each sample.

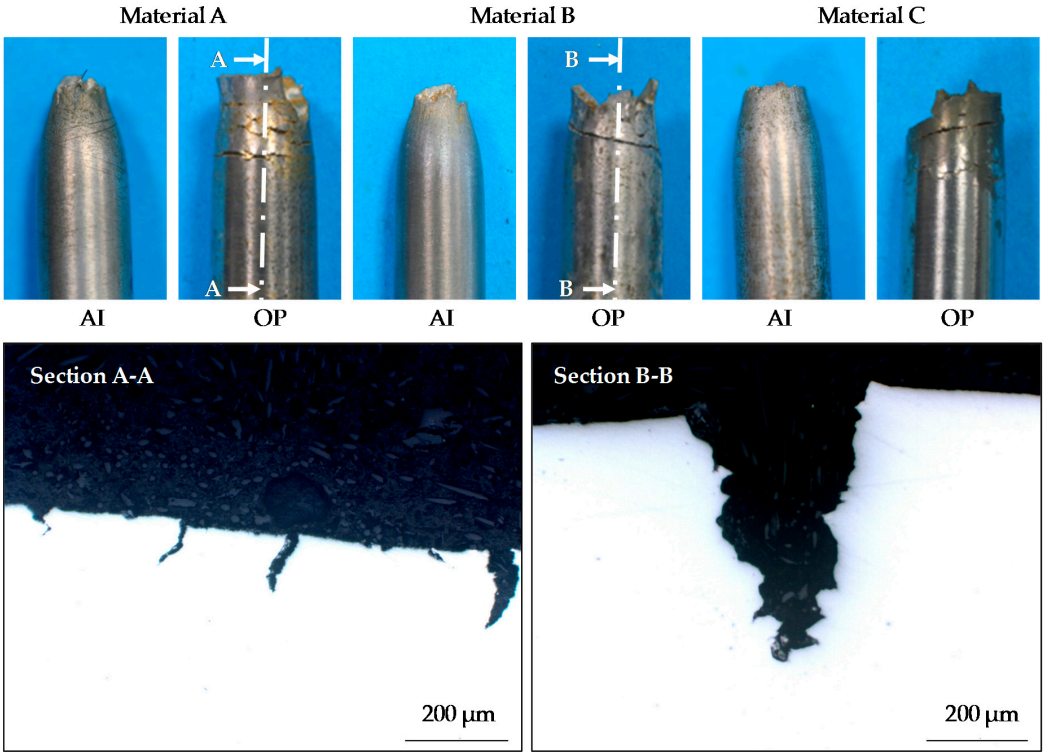

Figure 6. Top: Overview of the necking area of the specimens of each tested material in both extremes of HE aggressiveness (AI and OP); **Bottom**: Micrographs showing the surface cracks in the overprotected samples for materials A (multiple short cracks) and B (longer cracks but fewer) in the neighbourhood of the necking; both are resin mounted, polished down to Ra < 0.2 µm and un-etched.

4. Conclusions

The hydrogen embrittlement susceptibility of three high-strength mooring steels has been investigated with and without cathodic protection in cold and warm seawater, being the main conclusions:

- The three tested steels showed minor variations in the tests carried out in free corrosion conditions, both in cold and warm water, in comparison to the air condition.
- In consequence, the differences of SSRT HE ratios between tests in cold and warm seawater under cathodic protection are not related to temperature driven changes in the properties of the steels themselves, but of the testing environment. The R4 and R5 chain links showed a consistent improvement in the HE susceptibility ratios RE and RRA for the test in cold seawater when cathodic protection was applied.
- In terms of HE failure risk caused by cathodic overprotection, cold seas must thus be intrinsically less aggressive to the mooring chains than tropical seas. This fact underlines the importance of developing ad-hoc solutions for each mooring location, in which the temperature should be one of the parameters to be taken into account.
- The statement above is not applicable if a low HE sensitivity steel (such as the R4 accessory sample B) is employed for the mooring line. In this case, the effect of the seawater temperature has been found to be rather small.
- The R5 grade chain link sample showed a SSRT HE ratio comparable to the R4 chain link sample under cathodic protection (−850 mV), provided the ratios were normalized to the R4 chain accessory sample. This supports that HE susceptibility of higher strength grades doesn't necessarily have to increase, for normal cathodic protection, when compared to the results obtained for lower strength grades.

To sum up, the demand of improving the cost effectiveness of the offshore mooring systems employing high-strength chain steels will keep pulling the study of their differences in service behaviour among the diverse sea locations of industrial interest that can be found worldwide. Seawater temperature must be included in these chain link steel studies, not only because of its influence in bacterial growth and corrosion rates, but also for its contribution to HE kinetics when cathodic protection is applied.

Author Contributions: G.A. wrote the paper, designed the testing program and performed SSRT tests. A.A. coordinated the sample acquisition, specimen machining. He also prepared the experimental testing program and analysed tensile test results. A.F. optimised experimental setup for immersed tests and contributed reviewing the original manuscript. J.A. contributed with the writing of the paper and analysing SSRT results.

Funding: The authors acknowledge the financial support from the Spanish Ministry of Economy and Competitiveness through the project IPT-2012-1167-120000 with contribution from the European Regional Development Fund of the European Union (FEDER).

Acknowledgments: The authors would like to thank the project partners: Vicinay Cadenas, Gerdau Aceros Especiales, Institute of Construction Sciences "Eduardo Torroja" and Ik4-Tekniker.

Conflicts of Interest: The authors declare no conflicts of interest.

Abbreviations

HE	Hydrogen Embrittlement
SSRT	Slow Strain Rate Tensile
Rp0.2	Yield Strength
Rm	Ultimate Tensile Strength
E	Elongation
RA	Reduction in Area
AI	Test performed in air
FC-C	Test performed in seawater substitute under free corrosion in cold water (3 °C)
FC-W	Test performed under free corrosion in warm seawater substitute (23 °C)
CP-C	Test performed under a −850 mV cathodic protection in cold seawater substitute (3 °C)
CP-W	Test performed under a −850 mV cathodic protection in warm seawater substitute (23 °C)
OP-C	Test performed under a −1200 mV cathodic overprotection in cold seawater substitute (3 °C)
RECOND/CONT	Plastic Elongation Ratio where the subscript "COND" stands for the condition for which the ratio is calculated and "CONT" stands for the control condition employed for the calculation
RRACOND/CONT	Reduction in Area Ratio where the subscript "COND" stands for the condition for which the ratio is calculated and "CONT" stands for the control condition employed for the calculation

References

1. Billingham, J.; Sharp, J.V.; Spurrier, J.; Kilgallon, P.J. *Review of the Performance of High-Strength Steels Used Offshore*, 1st ed.; HSE Books: Sudbury, UK, 2003; ISBN 0-7176-2205-3.
2. Uno, N.; Kubota, M.; Nagata, M.; Tarui, T.; Kanisawa, H.; Azuma, K.; Miyagawa, T. Super-high-strength bolt "SHBT®". *Nippon Steel Tech. Rep.* **2008**, *97*, 95–104.
3. Louthan, M.R. Hydrogen embrittlement of metals: A Primer for the Failure Analyst. *J. Fail. Anal. Prev.* **2008**, *8*, 289–307. [CrossRef]
4. Peterson, I.M.; Sofronis, P.; Nagao, A.; Martin, M.L.; Wang, S.; Gross, D.W.; Nygren, K.E. Hydrogen embrittlement understood. *Metall. Mater. Trans. A* **2015**, *46A*, 2323–2341. [CrossRef]
5. Chung, Y.; Fulton, L.K. Environmental hydrogen embrittlement of G4140 and G4340 steel bolting in atmospheric versus immersion services. *J. Fail. Anal. Prev.* **2017**, *17*, 330–339. [CrossRef]
6. Sharp, J.V.; Billingham, J.; Robinson, M.J. The risk management of high-strength steels in jack-ups in seawater. *Mar. Struct.* **2001**, *14*, 537–551. [CrossRef]
7. Galvan, F.; Edwards, G.; Eren, E.; Slim, S. Acoustic emission technique to monitor crack growth in mooring chain. *J. Appl. Acoust.* **2018**, *139*, 156–164. [CrossRef]

8. DNVGL-CP-0237 Offshore Mooring Chain and Accessories, Class programme. Approval for Manufacturers. Available online: https://rules.dnvgl.com/docs/pdf/dnvgl/CP/2018-07/DNVGL-CP-0237.pdf (accessed on 16 July 2018).
9. *ASTM G129-00(2013), Standard Practice for Slow Strain Rate Testing to Evaluate the Susceptibility of Metallic Materials to Environmentally Assisted Cracking*; ASTM International: West Conshohocken, PA, USA, 2013. [CrossRef]
10. Nevshupa, R.; Martinez, I.; Ramos, S.; Arredondo, A. The effect of environmental variables on early corrosion of high-strength low-alloy mooring steel immersed in seawater. *Mar. Struct.* **2018**, *60*, 226–240. [CrossRef]
11. DNVGL-OS-E302 Offshore Mooring Chain, Offshore Standard. Available online: https://rules.dnvgl.com/docs/pdf/dnvgl/OS/2018-07/DNVGL-OS-E302.pdf (accessed on 16 July 2018).
12. Hong, X.; Xiangming, X.; Hua, L.; Sun, Y.; Dai, Y. Evaluation of hydrogen embrittlement susceptibility of temper embrittled 2.25Cr-1Mo steel by SSRT method. *J. Eng. Fail. Anal.* **2012**, *19*, 43–50. [CrossRef]
13. Li, X.; Zhang, J.; Ma, M.; Song, X. Effect of shot peening on hydrogen embrittlement of high-strength steel. *Int. J. Miner. Metall. Mater.* **2016**, *23*, 667–682. [CrossRef]
14. Akiyama, E.; Wang, M.; Li, S.; Zhang, Z.; Kimura, Y.; Uno, N.; Tsuzaki, K. Studies of evaluation of hydrogen embrittlement property of high-strength steel with consideration of the effect of atmospheric corrosion. *Metall. Mater. Tans. A* **2013**, *44A*, 1290–1300. [CrossRef]
15. Wang, M.; Akiyama, E.; Tsuzaki, K. Hydrogen degradation of a boron-bearing steel with 1050 and 1300 MPa strength levels. *Scr. Mat.* **2005**, *52*, 403–408. [CrossRef]
16. Artola, G.; Aldazabal, J. Estudio de agrietamiento en el ensayo SSRT de probetas galvanizadas. *Anal. Mech. Fract.* **2016**, *33*, 183–187. Available online: http://www.gef2016.es/docs/anales-de-mecanica-de-la-fractura-33.pdf (accessed on 16 July 2018).
17. Cabrini, M.; Pastore, M.; Bucella, D.P. Effect of Hot Mill Scale on Hydrogen Embrittlement of High-strength Steels for Pre-Stressed Concrete Structures. *Metals* **2018**, *8*, 158. [CrossRef]
18. Nagumo, M. *Fundamentals of Hydrogen Embrittlement*; Springer Science + Bussiness Media: Singapore, 2016; ISBN 978-981-10-0160-4.
19. McDougall, T.J.; Barker, P.M. Getting Started with TEOS-10 and the Gibbs Seawater (GSW) Oceanographic Toolbox. Available online: http://www.teos-10.org/pubs/Getting_Started.pdf (accessed on 16 July 2018).
20. Tromans, D. Temperature and pressure dependent solubility of oxygen in water: A Thermodynamic Analysis. *Hydrometallurgy* **1998**, *48*, 327–342. [CrossRef]
21. Hunter, K.A. The temperature dependence of pH in surface seawater. *Deep-Sea Res.* **1998**, *45*, 1919–1930. [CrossRef]
22. Ulfsbo, A.; Abbas, Z.; Turner, D.R. Activity coefficients of a simplified seawater electrolyte at varying salinity (5-40) and temperature (0 and 25 °C) using Monte Carlo simulations. *Mar. Chem.* **2015**, *171*, 78–86. [CrossRef]
23. DNVGL-RP-B401 Cathodic protection design, Recommended practice. Available online: https://www.dnvgl.com/oilgas/download/dnvgl-rp-b401-cathodic-protection-design.html (accessed on 16 July 2018).
24. Rizzo, P. NDE/SHM of underwater structures: A review. *Adv. Sci. Technol.* **2013**, *83*, 208–216. [CrossRef]
25. Angulo, A.; Allwright, J.; Mares, C.; Gan, T.; Soua, S. Finite element analysis of crack growth for structural health monitoring of mooring chains using ultrasonic guided waves and acoustic emission. *J. Procedia Struct. Integrity* **2017**, *5*, 217–224. [CrossRef]
26. Shukla, A.; Karki, H. Application of robotics in offshore oil and gas industry-A review Part II. *J. Robot. Autonom. Syst.* **2016**, *75*, 508–524. [CrossRef]